

Stylizing 3D Scene via Implicit Representation and HyperNetwork

PEI-ZE, CHIANG*, National Yang Ming Chiao Tung University, Taiwan
 MENG-SHIUN, TSAI*, National Yang Ming Chiao Tung University, Taiwan
 HUNG-YU, TSENG, University of California, Merced, USA
 WEI-SHENG, LAI, University of California, Merced, USA
 WEI-CHEN, CHIU, National Yang Ming Chiao Tung University, Taiwan

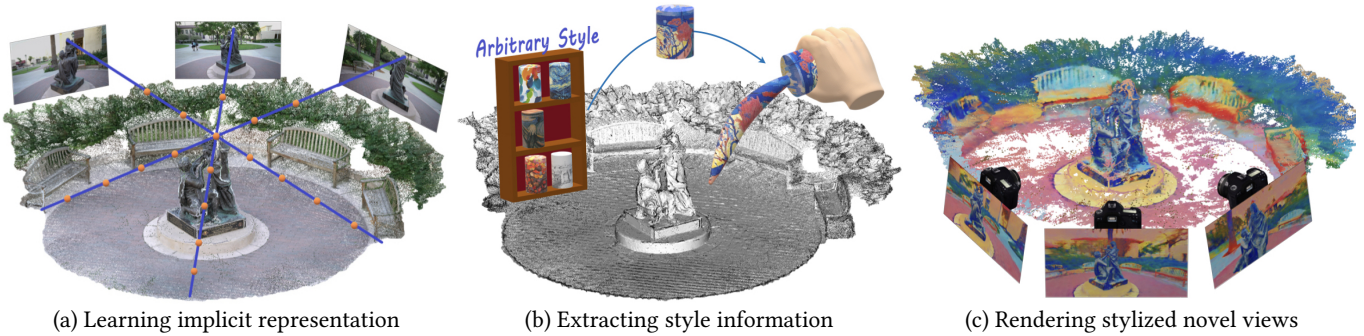


Fig. 1. **Transferring arbitrary styles to complex 3D scenes.** We propose a 3D scene style transfer approach that can render novel views with the desired style. (a) Our model first learns the implicit representation of a 3D scene and disentangles the geometry and appearance. (b) Then, the hypernetwork transfers the style information from the reference style image into the implicit scene representation. (c) Finally, our model is able to render novel views with consistent appearance at various view angles with arbitrary style.

In this work, we aim to address the 3D scene stylization problem - generating stylized images of the scene at arbitrary novel view angles. A straightforward solution is to combine existing novel view synthesis and image/video style transfer approaches, which often leads to blurry results or inconsistent appearance. Inspired by the high quality results of the neural radiance fields (NeRF) method, we propose a joint framework to directly render novel views with the desired style. Our framework consists of two components: an implicit representation of the 3D scene with the neural radiance field model, and a hypernetwork to transfer the style information into the scene representation. In particular, our implicit representation model disentangles the scene into the geometry and appearance branches, and the hypernetwork learns to predict the parameters of the appearance branch from the reference style image. To alleviate the training difficulties and memory burden, we propose a two-stage training procedure and a patch sub-sampling approach to optimize the style and content losses with the neural radiance field model. After optimization, our model is able to render consistent novel views at *arbitrary* view angles with *arbitrary* style. Both quantitative evaluation and human subject study have demonstrated that the proposed method generates faithful stylization results with consistent appearance across different views.

Authors' addresses: Pei-Ze, Chiang*, National Yang Ming Chiao Tung University, Taiwan; Meng-Shiun, Tsai*, National Yang Ming Chiao Tung University, Taiwan; Hung-Yu, Tseng, University of California, Merced, USA; Wei-sheng, Lai, University of California, Merced, USA; Wei-Chen, Chiu, National Yang Ming Chiao Tung University, Taiwan.

Permission to make digital or hard copies of all or part of this work for personal or classroom use is granted without fee provided that copies are not made or distributed for profit or commercial advantage and that copies bear this notice and the full citation on the first page. Copyrights for components of this work owned by others than ACM must be honored. Abstracting with credit is permitted. To copy otherwise, or republish, to post on servers or to redistribute to lists, requires prior specific permission and/or a fee. Request permissions from permissions@acm.org.

© 2021 Association for Computing Machinery.
 0730-0301/2021/5-ART \$15.00
<https://doi.org/10.1145/nnnnnnn.nnnnnnn>

CCS Concepts: • **Computing methodologies** → *Artificial intelligence*; **Computer vision**; **Computer vision tasks**;

Additional Key Words and Phrases: novel view synthesis, style transfer

ACM Reference Format:

Pei-Ze, Chiang*, Meng-Shiun, Tsai*, Hung-Yu, Tseng, Wei-sheng, Lai, and Wei-Chen, Chiu. 2021. Stylizing 3D Scene via Implicit Representation and HyperNetwork. *ACM Trans. Graph.* 1, 1 (May 2021), 12 pages. <https://doi.org/10.1145/nnnnnnn.nnnnnnn>

1 INTRODUCTION

This paper focuses on the problem of *stylizing the complex 3D scenes*. As demonstrated in Figure 1, given a set of example images of a 3D scene and a reference image with the desired artistic style, we aim to render consistent stylized images at arbitrary novel views. The proposed framework enables various virtual reality (VR) and augmented reality (AR) applications. For instance, with the growing popularity of virtual tours, our method enables seamless switching between real-world scenes and virtual artistic styles, such as walking through the River Seine under Van Gogh's starry night. On the other hand, one can preview a decorated house inside the VR world before doing the real painting work. 3D style transfer allows us to easily change the style of a scene and ensures the style consistency across view angles.

Numerous efforts have been made for controlling the appearance of the rendered 3D target. For instance, Xiang et al. [2021] and Kanazawa et al. [2018] formulate it as a texture synthesis problem.

* Both authors contributed equally to the paper

Specifically, they render the 3D objects with the desired texture by aligning the coordinates of the 2D UV (texture) map to those of the target object. However, these methods are designed specifically for a single object and are not capable of stylizing complex 3D scenes. On the other hand, the PSNet [Cao et al. 2020] method stylizes the point cloud of a 3D scene. Nevertheless, given the set of images of a 3D scene, it requires either the ground-truth 3D geometry or the estimated proxy geometry to build the point cloud. Moreover, the PSNet scheme suffers from the limited resolution issue due to the discrete characteristic of the point cloud representation. In contrast to point clouds that explicitly model 3D scenes, the recent neural radiance field (NeRF) [Mildenhall et al. 2020; Schwarz et al. 2020; Yu et al. 2021; Zhang et al. 2020] approaches introduce an implicit continuous volumetric representation that models a 3D scene using deep neural networks. Motivated by the high-quality novel view synthesis results, we aim to leverage neural radiance fields for transferring arbitrary styles to complex 3D scenes.

Leveraging neural radiance fields to stylize complex 3D scene is challenging for two reasons. First, neural radiance fields lack the controllability to manipulate the appearance of the 3D scene. Since the implicit continuous volumetric representation is built on the deep networks with millions of parameters, it is unclear which parameters control the style information of the 3D scene. To overcome this issue, one possible solution is combining existing image/video stylization approaches [Deng et al. 2021; Gao et al. 2020; Huang and Belongie 2017; Li et al. 2018, 2017b; Svoboda et al. 2020; Wang et al. 2020b] with novel view rendering techniques [Mildenhall et al. 2020; Zhang et al. 2020] by first rendering novel view images and then performing image stylization. However, as demonstrated in Figure 2, the current image/video stylization methods do not consider the consistency across different viewpoints for the same scene. We empirically show that the inconsistency issue leads to various problematic results in Section 4.

The second challenge is the memory limitation to apply the content and style losses [Li et al. 2017c] for learning stylization on the neural radiance field models. Note that these losses are computed across *holistic* images or patches in order to extract meaningful semantic features. However, in a neural radiance field model, it requires dense sampling along a camera ray to render a single pixel. It will take significantly more memory to render a patch for computing the losses and back-propagate the gradients. For example, it takes 17,934 MB for the NeRF [Mildenhall et al. 2020] model to render a patch of size 67×81 .

In this work, we propose a 3D scene style transfer approach based on neural radiance fields to address the above mentioned challenges. Our method is able to 1) transfer arbitrary styles to complex 3D scenes, and 2) be optimized with the commonly-used content and stylization losses. The proposed method consists of a neural radiance field model and a hypernetwork. Our neural radiance field model has two branches: a geometry branch and an appearance branch. We first optimize the neural radiance field model to reconstruct the input 3D scene, i.e., learn the implicit scene representation. Then, we fix the parameters of the geometry branch and optimize the hypernetwork to predict the parameters of the appearance branch in order to render the 3D scene with the style of the reference image. Moreover, to alleviate the GPU memory issue, we design a patch



Fig. 2. **Consistency issue of existing approaches.** Although we can attempt to stylize the complex 3D scene by combining the existing novel view synthesis (e.g. [Zhang et al. 2020]) and style transfer (e.g. [Huang and Belongie 2017]) methods, it produces inconsistent results across various viewpoints for the same scene. Note that the red boxes highlight the inconsistent appearance in the stylized results.

sub-sampling algorithm to train the hypernetwork using the content and stylization loss functions. After optimizing for a specific scene, our model is able to 1) render novel views with arbitrary and unseen styles, and 2) generate consistent stylization results across various viewpoints. We evaluate the proposed method with quantitative metrics (e.g., measuring the consistency of stylization across different viewpoints) and subjective user studies, which demonstrate that our method performs favorably against the baseline approaches on rendering more faithful and consistent stylization results.

The main contributions of this work include:

- We propose a 3D scene style transfer approach that can render novel views of a complex 3D scene with the desired style.
- We develop a hypernetwork to control the appearance-related weights of the neural radiance field model based on the given style image. Our model is universal and able to support arbitrary style images after optimization.
- We demonstrate that our method can synthesize faithful stylized images that are consistent across different view angles.

2 RELATED WORK

2.1 Novel View Synthesis

Novel view synthesis aims to synthesize a target image at an arbitrary camera pose from a set of source images. Conventional approaches [Fitzgibbon et al. 2005; Seitz et al. 2006; Sturm and Triggs 1996] often model a scene with *explicit* 3D representations, e.g., 3D meshes [Fua and Leclerc 1995] or 3D voxels [Kutulakos and Seitz 2000] based on the multi-view geometry. This line of work relies on a large number of source images to ensure the quality of 3D models. Recently, structure from motion [Schonberger and Frahm 2016] and multi-view stereo [Schönberger et al. 2016] techniques are also widely used to build up a 3D model. With the rapid advance of deep learning techniques, several recent approaches learn to estimate the 3D representation of a scene, such as mesh [Pontes et al. 2018], point cloud [Lin et al. 2018], and 3D voxel [Henderson and Ferrari 2019]. However, these methods require supervision from the ground-truth 3D representations and are only able to reconstruct a single object. Another group of works build the 3D representation without ground-truth supervisions. Image based rendering approaches [Riegler and Koltun 2020a,b] integrate the image features with the 3D proxy geometry (which is often reconstructed by multi-view stereo approaches), and then warp the input images to synthesize the target

view. Different from the explicit representations used in the above schemes, the neural radiance field approaches [Mildenhall et al. 2020; Yu et al. 2021; Zhang et al. 2020] encode the 3D scene information into multi-layer perceptron (MLP), which is an *implicit* 3D representation. This method takes the 3D coordinate and camera view direction as input to directly predict the RGB values and density, which does not rely on any pre-processing to obtain the proxy geometry. In this work, we also learn the implicit 3D representation using the neural radiance field model, but focus on transferring artistic styles to the rendered novel views.

2.2 Image and Video Style Transfer

Given a content image and a reference style image, the style transfer methods aim to synthesize an output image which shows the style of the reference image while preserving the structure of the content image. As a seminal work, Gatys et al. [2016] iteratively optimize the output image via a pre-trained deep network to render the desired style. Afterwards, several methods [Johnson et al. 2016; Li et al. 2017a; Ulyanov et al. 2016] develop feed-forward networks to significantly reduce the computational cost, but can only transfer a single or a set of pre-determined styles. To achieve arbitrary style transfer, recent frameworks use the adaptive instance normalization (AdaIN) [Huang and Belongie 2017], whitening and coloring transform (WCT) [Li et al. 2017b], or linear transformation (LST) [Li et al. 2018]. Recently, the TPFN [Svoboda et al. 2020] approach disentangles the image into a style and content codes, and designs a two-stage peer-regularized layer to transfer the target style information into the style code of the content image.

On the other hand, applying image style transfer approaches to a video frame-by-frame often results in temporal flickering and instability, as a small perturbation in the input frame may lead to significant changes in the stylized frame. Therefore, video style transfer methods focus on addressing the temporal consistency across the video footage. Existing methods introduce the optical flow to calculate temporal losses [Chen et al. 2017, 2020; Gupta et al. 2017] or align intermediate feature representations [Gao et al. 2018; Huang et al. 2017] in order to stabilize the model prediction across nearby video frames. Recent efforts further achieve consistent and real-time video style transfer through temporal regularization [Wang et al. 2020a,b], multi-channel correlation [Xia et al. 2021], and bilateral learning [Xia et al. 2021]. Although these methods have demonstrated impressive performance, they are design specifically for stylizing images or video sequences. Since the consistency across various viewpoints of the same scene is not considered, directly using existing image/video stylization schemes for our problem has various issues, as discussed in Figure 2 and Section 4.

2.3 Texture Transfer

Texture transfer aims to change the texture or style of a 3D object while keeping the appearance consistent across different view angles. Early works such as [Praun et al. 2000] attempt to create texture of the object surface meshes with the overlapping patches which are the copies of an example 2D texture. Such patch-based algorithms typically need particular design to avoid seams between patches and do not consider the texture synthesis from more holistic or global

perspective. With the recent advance of deep learning techniques, different methods [Groueix et al. 2018; Kanazawa et al. 2018; Xiang et al. 2021] are proposed to learn the correspondences between 3D shape (e.g. meshes) and the texture space for realizing the texture transfer. For instance, Xiang et al. [2021] learn a mapping from the implicit 3D representation to the 2D texture map, such that one can change the appearance of a 3D model by swapping the 2D texture map. However, such a texture mapping approach may generate unnatural results if the texture image is mapped across object edges or boundaries. In addition to texture mapping, recently there are several works [Cao et al. 2020; Kato et al. 2018] proposed to tackle the style transfer task on the 3D representations. For instance, Kato et al. [2018] propose to build a neural renderer where the rendering is integrated into neural networks, and demonstrate its application of style transfer on 3D models. PSNet [Cao et al. 2020] performs the style transfer on the point cloud data via manipulating the point cloud features in latent space to change the style. However, these methods rely on explicit 3D representations, such as mesh and point cloud, and are limited to the object level instead of the entire scene. Moreover, they do not support synthesizing stylized images with high-quality, which further limits their applications in the real world (e.g. AR). In this work, we resort to the *implicit* 3D scene representation and focus on transferring style for real-world 3D scenes with complex background, where the high-quality stylized novel views can be generated.

3 PROPOSED METHOD

Given a set of N images/photos $\{\mathcal{I}_n\}_{n=1}^N$ of a static 3D scene taken from different camera poses $\{(R_n, t_n)\}_{n=1}^N$, our goal is to render arbitrary novel views of the 3D scene with the style extracted from a reference image S . The rendered images should have consistent texture and stylization effect across different views. To this end, we propose a 3D style transfer method to enable the universal stylization of a complex 3D scene. We model a 3D scene with implicit representation by the neural radiance fields (Section 3.1), and learn to transfer arbitrary style using a hypernetwork (Section 3.2). To alleviate the training difficulties, we propose a two-stage training pipeline, where the geometric training stage learns the implicit representation of a 3D scene by disentangling the geometry and appearance into two branches, and the stylization training stage learns to predict the parameters of the appearance branches from the reference image S (Section 3.3).

3.1 Preliminaries

The model of neural radiance fields (i.e. NeRF) proposed in [Mildenhall et al. 2020] adopts a sparse set of input views of a 3D scene for learning to optimize the underlying continuous volumetric scene function. The basic idea behind NeRF can be illustrated as in Figure 3(a). Given a camera observing the 3D scene at the viewing direction $d = (\theta, \phi)$, we first march along the rays back-projected from the camera center through all the pixels on the image plane for obtaining the samples of 3D points $x = (x, y, z)$. The scene function as an implicit scene representation then takes both x and d as input to output the volume density σ at x and the corresponding RGB color $c = (r, g, b)$ emitted towards the viewing direction d . To be

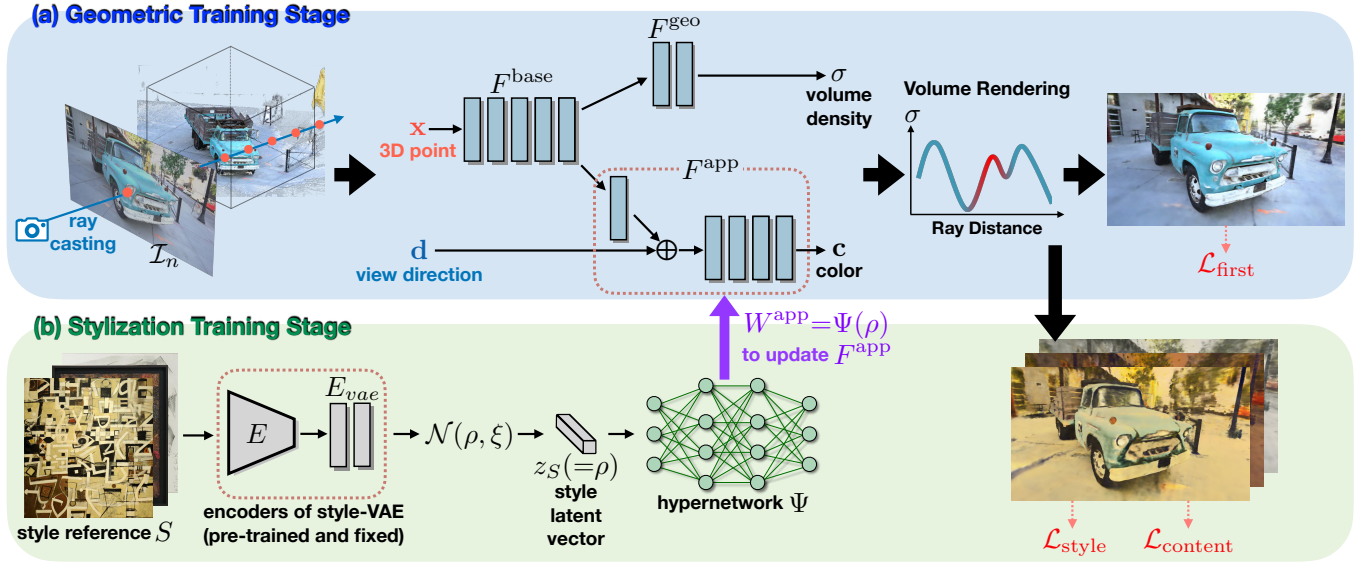


Fig. 3. **Algorithmic overview.** The proposed framework consists of a neural radiance field model with a geometry branch (i.e. F^{base} together with F^{geo}) as well as an appearance branch (i.e. F^{app}), and a hypernetwork Ψ . (a) Firstly in the geometric training stage it learns to reconstruct the target 3D scene from a set of input images $\{I_n\}_{n=1}^N$. (b) Then in the stylization training stage, it learns to transfer arbitrary styles. We keep the geometry branch fixed, and optimize the hypernetwork Ψ to predict the parameters W^{app} in the appearance branch according to the style latent vector z_S extracted from the input reference (style) image S . After the two-stage optimization, we can render images with desired style at arbitrary novel views using volume rendering.

detailed, the scene function consists of three multilayer Perceptrons (MLPs): F^{base} , F^{geo} , and F^{app} . In practice, F^{base} takes x as input where the produced $F^{\text{base}}(x)$ is either passed through F^{geo} to obtain the volume density σ , or further processed by F^{app} together with d to obtain the view-dependent color c via $F^{\text{app}}(F^{\text{base}}(x), d)$. With accumulating the colors and densities via the volume rendering techniques, the high-quality 2D images as the observation of the 3D scene from various views can be generated. Please note that, in practical implementation [Mildenhall et al. 2020] both x and d are firstly transformed into positional embeddings before being utilized by the MLPs (i.e. F^{base} and F^{app}).

While the original NeRF model seems to demonstrate compelling capability in the view synthesis, when it is adopted to tackle the 360° captures of unbounded and complex scenes, simultaneously modelling the the nearby and far objects (related to foreground and background respectively) by the same volumetric scene function would cause problems for volume rendering as being required to handle the large dynamic depth range between objects, as pointed out by [Zhang et al. 2020]. Hence, for the rendered images, there could exist significant artifacts in the background if only a portion of the scene (mainly the foreground objects) is modelled, while missing the image details once attempting to model the full scene. In order to deal with such issue, NeRF++ [Zhang et al. 2020] separates the foreground and background objects into the inner volume and outer volume by a unit sphere, with having two NeRFs adopted to model them respectively, where an inverted sphere parameterization is particularly applied on the coordinate system of outer volume for bounding the potentially unlimited distance between the background objects and the origin. In our work, we hence adopt the

model of NeRF++ [Zhang et al. 2020] to represent the unbounded and complex 3D scenes.

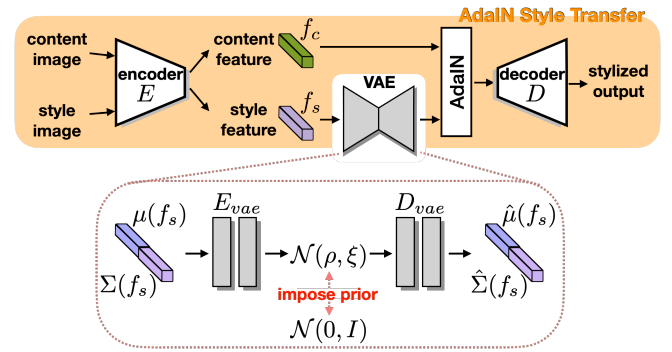


Fig. 4. Illustration of pre-training of the the style variational autoencoder (style-VAE) model. Built upon the AdalN framework [Huang and Belongie 2017] of image style transfer, a variational autoencoder [Kingma and Welling 2014] learns to project the style features f_s into the latent style vectors, where the distribution of latent style vectors is regularized to follow a normal distribution for the purpose of enabling universal stylization. Please refer to Section 3.2 for more details.

3.2 Stylization on NeRF-based Scene Representation

Without loss of generality, the operation of style transfer aims to keep the geometry/content of the target scene while modifying its appearance/texture according to the reference style image. From the design of NeRF models, we can see that the geometry and the

appearance information of the scene are respectively represented by the volume densities and the view-dependent color values at each 3D location. Therefore, in order to stylize the 3D scene implicitly encoded by NeRF, we propose a novel approach to modify the parameters/weights of the MLP F^{app} (i.e. **appearance branch**) which is responsible for predicting the color values, while keeping the other MLPs (i.e. F^{base} and F^{geo} , the **geometry branch**) fixed in order to retain the geometry of the target scene. Basically, our stylization method on the NeRF-based scene representation is realized by two components: the **style variational autoencoder** to extract the style latent vector z_S from the reference style image S , and the **hypernetwork** Ψ to estimate the weights for modifying F^{app} according to z_S . We detail these two components in the following.

Hypernetwork. As illustrated in Figure 3(b), given a style latent vector z_S extracted from the style reference image S , the hypernetwork Ψ (built upon a MLP in our work) learns to regress from z_S to produce the weights W^{app} for updating F^{app} , in which the updated F^{app} (denoted as \tilde{F}^{app}) is then able to predict the color value emitted from 3D location \mathbf{x} toward view direction \mathbf{d} , and the resultant images of view synthesis after running volume rendering are expected to have the style as S . Please note that, the idea of hypernetwork (i.e. regressing the network parameters via another network) was originally proposed in [Ha et al. 2016] but we innovatively adopt it here for the task the 3D scene stylization.

Style Variational Autoencoder. Instead of merely having our stylization effective for limited number of styles which are seen during hypernetwork learning, we aim to achieve the **universal stylization** thus being able to render scene images with arbitrary and unseen styles in the inference/testing time. To this end, we propose the style variational autoencoder (style-VAE) to regularize the distribution of style latent vectors into a normal distribution, and expect that the hypernetwork Φ is generalizable to the unseen styles.

The architecture of our style-VAE is illustrated in Figure 4, where we extend from the well-known AdaIN framework [Huang and Belongie 2017] of image style transfer to additionally equip a variational autoencoder (VAE [Kingma and Welling 2014]) into the space of style features f_s extracted from style reference images S by an ImageNet-pretrained VGG-19 encoder E [Simonyan and Zisserman 2015]. Basically, such variation autoencoder is composed of an encoder E_{vae} and a decoder D_{vae} (both built upon MLPs), where E_{vae} encodes $\{\mu(f_s), \Sigma(f_s)\}$ (i.e. the mean and standard deviation of style feature f_s) into a Gaussian distribution $\mathcal{N}(\rho, \xi)$ and D_{vae} decodes from $\epsilon \sim \mathcal{N}(\rho, \xi)$ to produce the reconstructed $\{\hat{\mu}(f_s), \hat{\Sigma}(f_s)\}$. Note that, we use ρ obtained from $E_{vae}(\{\mu(E(S)), \Sigma(E(S))\})$ as the style latent vector z_S of the style reference image S . Afterwards, $\{\hat{\mu}(f_s), \hat{\Sigma}(f_s)\}$ are used to perform the adaptive instance normalization on the content feature f_c (extracted from the content image by E) for realizing the image style transfer on the content image as what the typical AdaIN framework does.

The learning objective of our style-VAE simply includes the loss functions for training the typical AdaIN and VAE frameworks, i.e. the content loss and style loss from AdaIN [Huang and Belongie 2017], as well as the reconstruction loss (between $\{\mu(f_s), \Sigma(f_s)\}$ and $\{\hat{\mu}(f_s), \hat{\Sigma}(f_s)\}$) and the KL-divergence loss on $\mathcal{N}(\rho, \xi)$ from

VAE [Kingma and Welling 2014]. In particular, the KL-divergence loss regularizes the distribution of latent style vectors to follow the normal distribution. While having sufficient number of training styles for learning the hypernetwork Ψ , we expect that the latent style vectors of unseen styles which are projected into the same latent distribution can be well handled by the hypernetwork thus producing the plausible W^{app} for driving the scene stylization. Please note that, as the style-VAE aims for learning to extract the latent style vectors from the style reference images where none of its objective functions is related to the stylization part, it thus can be learnt beforehand and kept fixed during training our scene stylization model.

3.3 Model Training

The training procedure for our 3D scene style transfer approach contains the geometric training and the stylization training stages. We describe these two stages and the corresponding objective functions in the following.

Geometric training stage (first stage). In this stage we aim to learn the NeRF-based representation of the target 3D scene from the given N images $\{I_n\}_{n=1}^N$ taken from different camera poses $\{(R_n, t_n)\}_{n=1}^N$. The NeRF++ [Zhang et al. 2020] model is adopted and its training process is briefly summarized as follows. At each optimization iteration, we randomly sample M pixels from input images to form a batch of camera rays $\{r_m\}_{m=1}^M$ and 3D points (marching along the rays) based on the corresponding camera poses and the camera intrinsic. With taking these 3D points and their corresponding view directions (i.e. the directions of the corresponding camera rays) as input to the scene function of NeRF to obtain the output set of volume densities and colors, the volume rendering technique is used to render the color value $\hat{c}(r_m)$ of each ray r . The objective for training the MLPs of the scene function (i.e. F^{base} , F^{geo} , and F^{app}) is the squared error between $\hat{c}(r_m)$ and the groundtruth color $c(r_m)$ of the corresponding image pixel of ray r_m .

$$\mathcal{L}_{\text{first}} = \sum_{m=1}^M \|\hat{c}(r_m) - c(r_m)\|_2 \quad (1)$$

Stylization training stage (second stage). As in the previous geometric training stage we have encoded the complete geometry and the original appearance of the target 3D scene into the NeRF model, now in the stylization training stage we will focus on learning the hypernetwork Ψ to predict from the style latent vector z_S the weights W^{app} for updating MLP F^{app} , where z_S is extracted from the style reference image S by the pretrained encoders of style-VAE, i.e. $E_{vae}(\{\mu(E(S)), \Sigma(E(S))\})$. Note that as the geometry of the 3D scene should be retained during the stylization, both F^{base} and F^{geo} are kept fixed during this training stage.

As the goal of our style transfer is to stylize the whole scene such that the generated images of view synthesis are able to demonstrate the similar style as the reference S , ideally we should render the holistic images or patches to compute of typical content and style losses [Huang and Belongie 2017], which are widely used in style transfer works, for validating the effectiveness of stylization. However, since rendering a single pixel already needs dense sampling

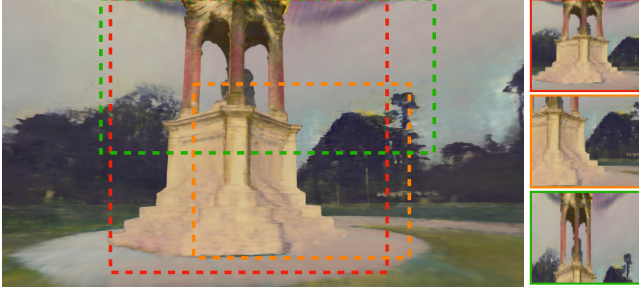


Fig. 5. **Patch sub-sampling.** Instead of using the holistic novel view image, we design a patch sub-sampling algorithm to reduce the computation of the content loss $\mathcal{L}_{\text{content}}$ and style loss $\mathcal{L}_{\text{style}}$. For each novel view image, we obtain a sub-sampling region by randomly determining the position and the size of the region, i.e., the dash-lined boxes. We then extract and resize the region using nearest neighbor sub-sampling to get the small patch with fixed size, as the three patches shown in the right. Finally, we use the patches to compute the losses for stylization.

on the camera ray to obtain numerous 3D points for querying the NeRF model, it would be even more costly in terms of GPU memory usage when attempting to render the holistic image/patch and perform the back-propagation for network optimization. In order to tackle such issue, we propose a **patch sub-sampling** algorithm to enable the computation of content and style losses: As illustrated in Figure 5, a random window is firstly cropped from the input image with having the height and width of such window at least larger than a ratio (Λ_w and Λ_h respectively) of the input image size, then we uniformly sample $\eta_w \times \eta_h$ pixels from such window to form a smaller image patch (where the number of pixels is constrained by the GPU memory). By using our patch sub-sampling algorithm to select the patch $P(\mathcal{I}_n)$ from input image \mathcal{I}_n and its paired patch $P(\tilde{\mathcal{I}}_n)$ from the stylization result $\tilde{\mathcal{I}}_n$, the content and style losses are computed between them.

In details, the content loss $\mathcal{L}_{\text{content}}$ encourages $P(\mathcal{I}_n)$ and $P(\tilde{\mathcal{I}}_n)$ to have the similar content features:

$$\mathcal{L}_{\text{content}} = \left\| \tau(P(\mathcal{I}_n)) - \tau(P(\tilde{\mathcal{I}}_n)) \right\|_2 \quad (2)$$

where $\tau(\cdot)$ denotes the feature representation obtained from the `relu4_1` layer of a ImageNet-pretrained VGG-19 network. And the style loss $\mathcal{L}_{\text{style}}$ measures the mean squared error in term of feature statistics between $P(\tilde{\mathcal{I}}_n)$ and the reference style image S , which is defined as:

$$\begin{aligned} \mathcal{L}_{\text{style}} = & \sum_l \left\| \mu(\tau_l(S)) - \mu(\tau_l(P(\tilde{\mathcal{I}}_n))) \right\|_2 \\ & + \sum_l \left\| \Sigma(\tau_l(S)) - \Sigma(\tau_l(P(\tilde{\mathcal{I}}_n))) \right\|_2 \end{aligned}$$

where μ and Σ denote the mean and standard deviation respectively, and $\tau_l(\cdot)$ denotes the feature representation obtained from the l -th layer of a ImageNet-pretrained VGG-19 network, basically `relu1_1`, `relu2_1`, `relu3_1`, and `relu4_1` layers are used.

The overall objective function for the stylization training stage, in which the gradients are back-propagated to learn the hypernetwork

Ψ , is then defined as:

$$\mathcal{L}_{\text{second}} = \mathcal{L}_{\text{content}} + \lambda_{\text{style}} \mathcal{L}_{\text{style}} \quad (3)$$

where the hyperparameter λ_{style} controls the balance between the content loss and style loss, and we set $\lambda_{\text{style}} = 15$ for all our experiments.

Implementation details. In the geometric training stage, our NeRF model is trained for 250,000 iterations, while in the stylization training stage, our hypernetwork Ψ is trained for 100,000 iterations, where in the first 2,000 only the content loss is used for having better initialization of the hypernetwork. We adopt the Adam optimizer for both stages with learning rates set to 0.0005 and 0.001 respectively. Moreover, in the geometric training stage, we set $M = 67 \times 81$; while in the stylization training stage, we have Λ_w , Λ_h , η_w , and η_h set to 1/3, 1/2, 81, and 67 respectively. Following [Shen et al. 2018], each style reference image used in our experiments is resized to keep the smallest dimension in the range [256, 480], and randomly cropped regions of size 256×256 .

4 EXPERIMENTAL RESULTS AND ANALYSIS

In this section, we present qualitative and quantitative results to validate the effectiveness of our proposed framework. Please refer to the supplementary materials for more qualitative results. We will release the source code and pre-trained model on our project page¹ to stimulate further research in this field.

Datasets. We conduct the experiments using five real-world 3D scenes collected in the Temples and Temples [Knapitsch et al. 2017] dataset, i.e., Family, Francis, Horse, Playground and Truck. During the geometric training stage, we follow [Mildenhall et al. 2020] to use the COLMAP SfM [Schonberger and Frahm 2016] method to estimate the camera poses and intrinsics of the input images for each 3D scene. On the other hand, we use 81330 images in the WikiArt dataset [Nichol 2016] as the reference style images. Specifically, we randomly select 112 images as the testing data and keep the others for the stylization training stage.

Compared methods. To the best of our knowledge, there is no existing method that focuses on stylizing complex 3D scenes. Therefore, we combine different image/video stylization methods with the novel view synthesis algorithms to build three types of baseline approaches:

- Image stylization \rightarrow novel view synthesis: we stylize the input images of the target scene, then perform novel view synthesis.
- Novel view synthesis \rightarrow image stylization: we perform image stylization on the novel view synthesis results.
- Novel view synthesis \rightarrow video stylization: we treat a series of novel view synthesis results (generally along a smooth camera path) as the *video*, then perform video stylization.

Specifically, we use neural radiance field model described in Figure 3 (a) as the novel view synthesis approach. The AdaIN [Huang and Belongie 2017], WCT [Li et al. 2017b], LST [Li et al. 2018], and

¹ Project page: <https://ztex08010518.github.io/3dstyletransfer/>

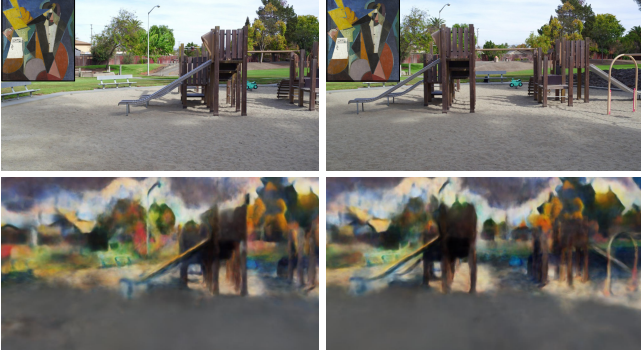


Fig. 6. **Qualitative results of “image stylization → novel view synthesis” baseline.** Since the input images of the target 3D scene are stylized independently by the AdaIN [Huang and Belongie 2017] approach, these images are not consistent across different views. As a result, the novel view synthesis algorithm blends such inconsistency and produces blurry results.

TPFR [Svoboda et al. 2020] schemes are used for image stylization. Finally, we use two video stylization frameworks, i.e., ReReVST [Wang et al. 2020b] and MCCNet [Deng et al. 2021].

4.1 Qualitative Results

We present the qualitative comparisons in Figure 6 and Figure 12. The baseline “image stylization → novel view synthesis” produces blurry results, as shown in Figure 6. Since the input images are processed independently by the AdaIN [Huang and Belongie 2017] approach, the stylized images are not consistent across different views of the same scene. Therefore, the optimization of the neural radiance field model with these inconsistent images leads to the blurry results. Moreover, as the neural radiance field model is optimized for a specific style, this baseline method is not capable of transferring arbitrary style to the 3D scene. On the other hand, the baseline “novel view synthesis → image stylization” also produces inconsistent results across different viewpoints, as highlighted in the red boxes in Figure 12. In particular, the baseline based on the WCT [Li et al. 2017b] approach fails to preserve the content of the original 3D scene, while the another one based on the TPFR [Svoboda et al. 2020] scheme does not transfer the desired style provided by the reference image. In contrast, the results synthesized by our method not only match the desired style, but also are consistent across various novel views. More stylized results of our proposed method are provided in Figure 11 and the supplementary materials.

We demonstrate the qualitative results by the baseline “novel view synthesis → video stylization” in the lower half of Figure 12. Although these video-stylization-based methods are trained to consider the *short-term* consistency, they fail to produce consistent results between two far-away viewpoints due to the error accumulation, e.g., the head and the back of the statue. In contrast, since our framework is trained to stylize the holistic 3D scene, it generates the results that are consistent between both short-range or long-range viewpoints.

4.2 Quantitative Results

User preference study. In order to evaluate the quality of stylizing complex 3D scenes, we conduct a study to understand the user preference between the results rendered by the proposed and baseline methods. Note here we focus on the comparison against “novel view synthesis → image stylization” and “novel view synthesis → video stylization” baselines as the “image stylization → novel view synthesis” ones generally produce too blurry results as shown in Figure 6.

Specifically, we use a series of stylized novel view synthesis results (along a smooth camera path) to create a video. For each 3D scene, we present two videos produced by different approaches, and ask the user to select the one that 1) better matches the given reference style image and 2) shows less flickering, i.e. being more consistent between different views. There are 73 users participated in this study. For each user, there are 2 tests conducted for each comparison (i.e. proposed method versus one baseline in terms of stylization quality or temporal consistency). The results are demonstrated in Figure 7. The proposed method performs favorably against the baseline schemes in terms of both the stylization quality and consistency. We also observe that the “novel view synthesis → video stylization” baseline produce videos with less flickering compared to the “novel view synthesis → image stylization” ones since they consider the temporal consistency. However, these approaches fail to preserve the consistency between two far-away viewpoints, as demonstrated in the following experiments.

Consistency. In addition to the user preference study that evaluates the quality of the stylization results, we use the metric from Lai et al. [2018] to measure the consistency between different stylized novel view images. Specifically, for two stylized images \tilde{I}_u and \tilde{I}_v at novel views u and v , we use their corresponding ground-truth *non-stylized* images I_u and I_v to compute the optical flow, as well as the occlusion mask O . Specifically, we use the pre-trained FlowNet 2.0 [Ilg et al. 2017] to obtain the optical flow. According to the computed optical flow, we warp the stylized image \tilde{I}_v at the view v to get the corresponding image \tilde{I}_u at the view u . Finally, the consistency metric is computed as

$$\mathcal{E}_{\text{consistency}}(\tilde{I}_u, \tilde{I}_v) = \frac{1}{|O|} \left\| \tilde{I}_u - \tilde{I}_u \right\|_2^2 \quad (4)$$

where $|O|$ denotes the number of non-occluded pixels in O .

In the following experiments, we evaluate the consistency from two different perspectives: 1) the *short-range* consistency between to nearby novel views, and 2) the *long-range* consistency between to far-away novel views.

Table 1 shows the short-range consistency scores. In this experiment, we use every two adjacent novel views, i.e., the $t - th$ and $(t - 1) - th$ frames in the testing video, to compute the consistency score. We observe that the results generated by the image stylization baseline methods are not consistent as the novel view images are processed independently. Moreover, while the TPFR [Svoboda et al. 2020] approach achieves lowest scores among all the baseline schemes, it however fails to capture of desired style of the reference image in some cases, as shown in Figure 12.

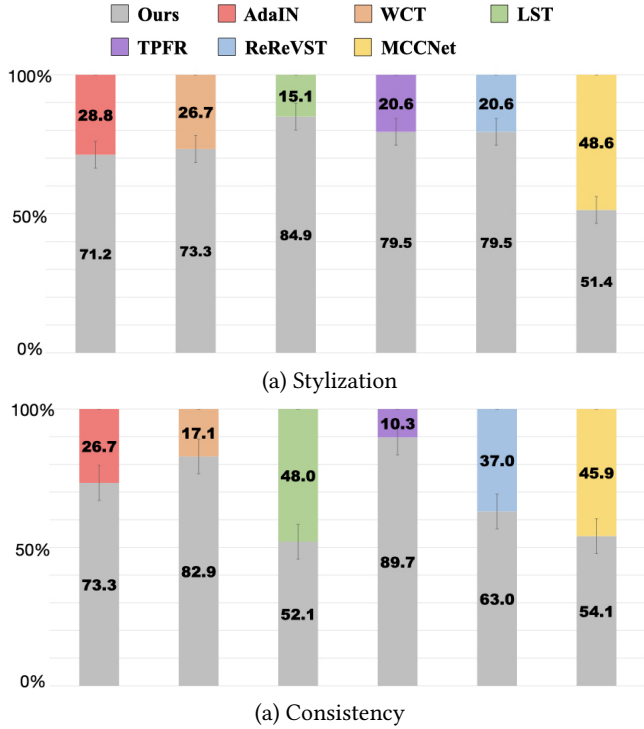


Fig. 7. **User preference study.** In this study, we present two novel view synthesis results (created as videos) generated by different methods, and ask the user to select the one that 1) matches the given reference (style) image and 2) shows less flickering (i.e., mode consistent).

Table 1. **Qualitative comparisons on short-range consistency.** We compute the consistency score $\mathcal{E}_{\text{consistency}}$ (the lower the better) between stylized images at two adjacent novel views.

Methods	Family	Francis	Horse	Playground	Truck	Average
AdaIN	2.0172	1.9015	2.5102	1.7011	1.8582	1.9976
WCT	2.9717	2.8170	3.5992	2.5998	3.0162	3.0008
LST	4.3897	3.2608	4.0586	3.1262	3.6980	3.7067
TPFR	1.0930	0.6611	1.2504	0.6448	0.6908	0.8680
ReReVST	1.0089	0.8431	1.3006	0.6404	0.8617	0.9309
MCCNet	1.1006	0.8334	1.4186	0.9609	1.1359	1.0899
Ours	0.2885	0.2653	0.4127	0.2708	0.2735	0.3022

We present the long-range consistency score in Table 2. Specifically, we use every two far-away views, i.e., the $t - th$ and $(t - 7) - th$ frames in the testing videos, to compute the consistency score. Since the distance between two views are larger, the consistency scores of all methods in this experiment are higher than those in the short-range study. Although the video stylization baselines generally better preserves the short-range consistency than the image stylization ones, they fail to maintain the consistency between two far-away views due to the error accumulation. In contrast, the proposed

Table 2. **Qualitative comparisons on long-range consistency.** We compute the consistency score $\mathcal{E}_{\text{consistency}}$ (the lower the better) between stylized images at two far-away novel views.

Methods	Family	Francis	Horse	Playground	Truck	Average
AdaIN	6.4704	5.5091	5.5914	6.4771	5.2145	5.8526
WCT	6.7233	6.2752	6.8781	6.3403	6.6640	6.5767
LST	8.0778	6.1186	8.1056	8.6210	9.3647	8.0575
TPFR	4.2423	2.5301	5.0199	5.1047	3.1312	4.0056
ReReVST	4.8321	4.5702	4.3904	5.8077	4.4881	4.8177
MCCNet	5.7786	4.1305	4.6071	5.3677	4.7280	4.9224
Ours	3.5101	2.8598	2.5637	3.2701	2.7423	2.9892

method is capable of synthesizing images that are both short-range and long-range consistent.

4.3 Ablation Study

In this section, we present the ablation study results to further understand the effectiveness of the proposed framework.

Numbers of training style images. In the previous experiments, we use 81330 style images to train the hypernetwork for universal stylization. In this experiment, we demonstrate the generalization ability of the proposed framework by lowering the number of training style images. As shown in Figure 8, the proposed hypernetwork trained with 200 or 2000 style images is still able to produce appealing stylization results.

Joint training vs. proposed two-stage training strategy. As described in Section 3.3, we design a two-stage training strategy to train the proposed model for stylizing a particular 3D scene. In this experiment, we validate the importance of the two-stage training strategy by comparing with the model jointly trained with $\mathcal{L}_{\text{first}}$ and $\mathcal{L}_{\text{second}}$ which are described in Section 3.3. We present the results in Figure 9. The joint training strategy is a more complicated learning task since it involves the construction of the target 3D scene, and the learning of the stylization. As a result, the proposed model trained with the joint training strategy fails to render the desired style as well as the correct geometry. In contrast, we develop the two-stage training strategy to simplify the training task that the geometry branch is first optimized to model the target 3D scene, the hypernetwork is trained for the universal stylization.

4.4 Limitations

There are several limitations in the proposed framework. First, the quality of the stylization results is limited by the backbone neural radiance field model. As the red boxes shown in Figure 10, the proposed method produces blurry stylization results since the backbone neural radiance field model fails to capture the details of the trees. In contrast, the details of both the original and stylized wheels demonstrated in the green boxes are clear. Second, the optimization and the inference of the neural radiance field model are computationally demanding and time-consuming. Specifically, the proposed framework requires two days for the optimization (the geometric and stylization training stages), and 70 seconds for rendering a

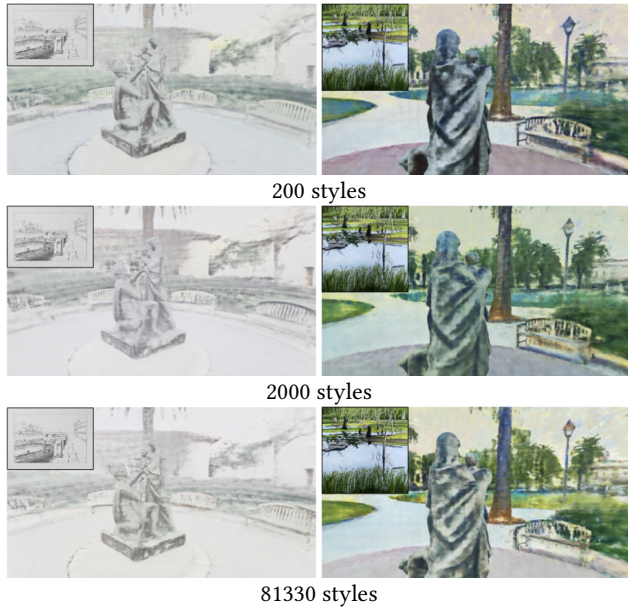


Fig. 8. **Study on number of style images used for the stylization training stage.** We present the example stylization results based on the unseen style (shown on the top-left corner of each example) by using the hypernetwork with 81330, 2000 and 200 style images. Note that we use the same training hyper-parameters (e.g., learning rate) except the number of training images in this experiment.

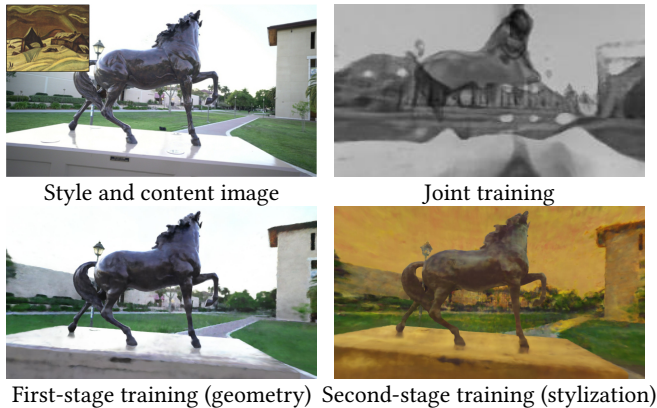


Fig. 9. **Importance of the two-stage optimization strategy.** To understand the importance of our two-stage training strategy (as described in Section 3.3), we present the results of optimizing the proposed model in a single-stage, i.e., joint training with using losses $\mathcal{L}_{\text{first}}$ and $\mathcal{L}_{\text{second}}$ at the same time. The proposed approach fails to capture the geometry of the target scene and render the images with desired style while not adopting the proposed two-stage strategy.

1084×1957 image. In the coming future, we plan to explore the solutions that accelerate the training and inference processes, e.g., FastNeRF [Garbin et al. 2021].

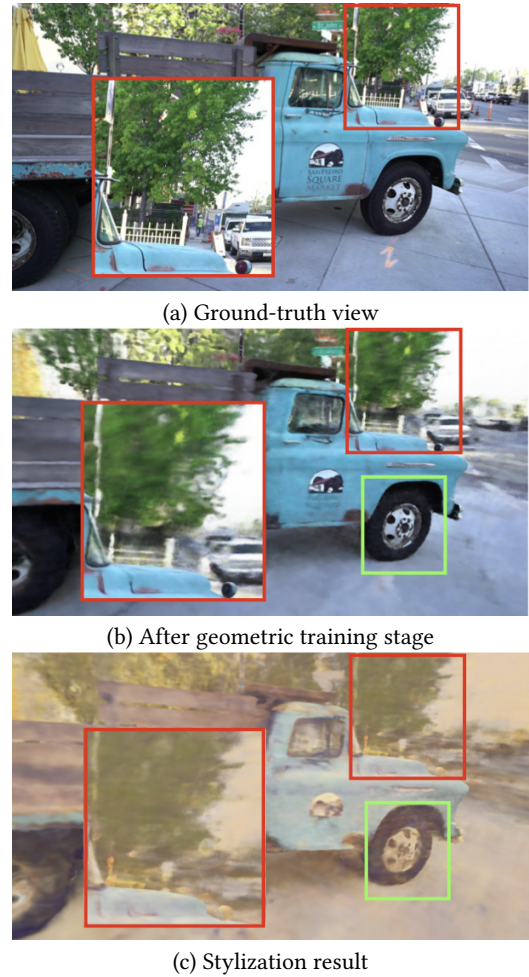


Fig. 10. **Failure cases.** The propose approach is limited by the backbone neural radiance field model. The red boxes demonstrate that if the backbone model fails to capture the detail, the stylization results are also blurry. In contrast, the green boxes show a positive example that the details are clear.

5 CONCLUSIONS

In this paper, we propose a neural radiance field model for transferring arbitrary styles to complex 3D scenes. We design a hypernetwork to predict the appearance-related parameters in the neural radiance field model to stylize the 3D scene according to the input reference (style) image. In addition, we develop a two-stage training strategy along with the sub-sampling algorithm to learn the hypernetwork. Qualitative and quantitative results validate that the proposed method renders high-quality novel view images with the desired style.

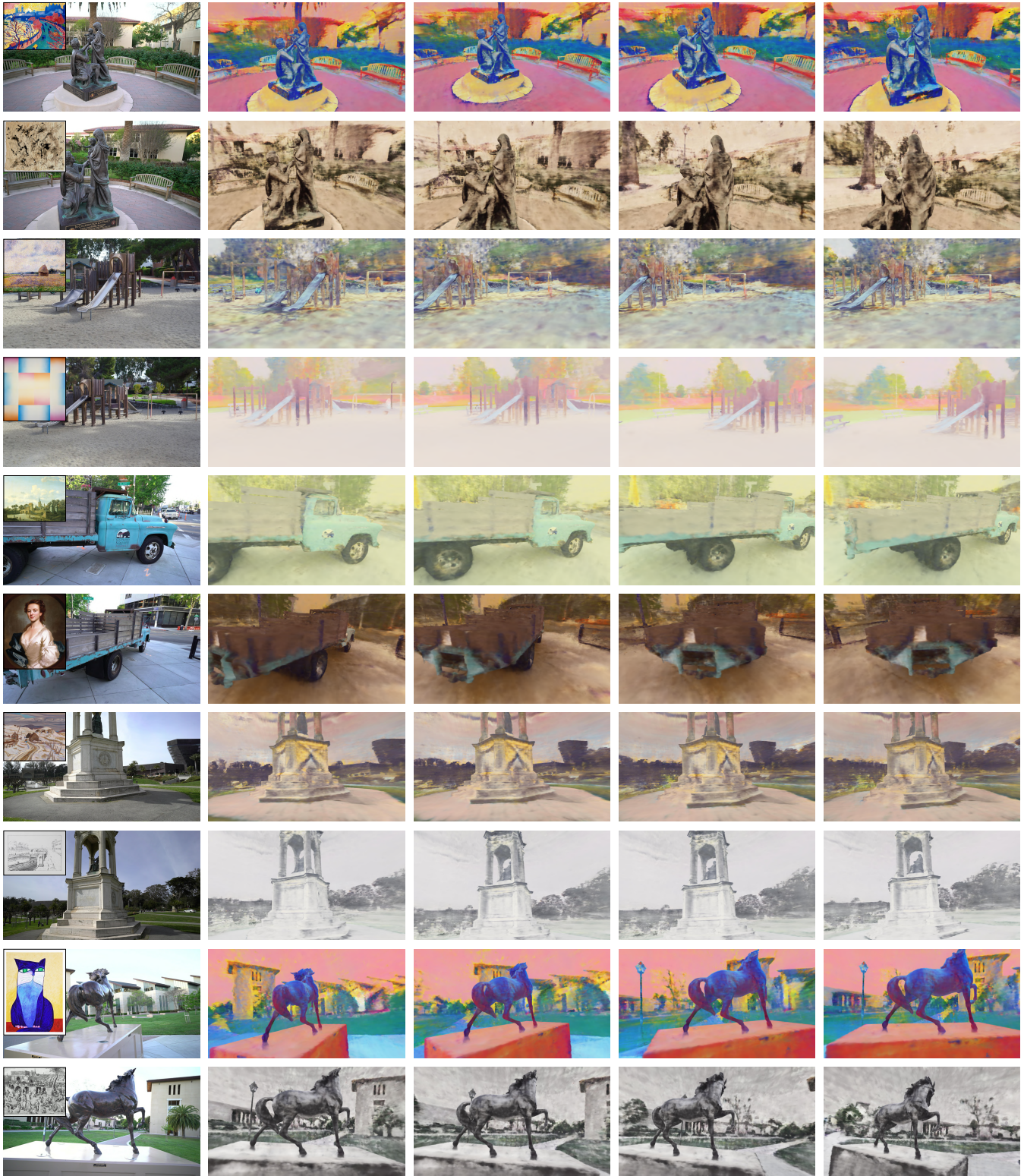


Fig. 11. **Qualitative results of our proposed framework of 3D scene stylization.** For each row, the leftmost column presents an example input image of the scene together with the input reference (style) image on the top-left corner, while the remaining columns demonstrate the stylization results at various novel views.



Fig. 12. **Qualitative comparisons.** The top row presents example input images of two scenes with their corresponding input reference (style) images shown on the top-left corner. Our proposed approach renders images (shown in the last row) which contain desired style and are consistent across different view angles. The red boxes highlight the inconsistent stylization across different views.

REFERENCES

- Xu Cao, Weimin Wang, Katashi Nagao, and Ryosuke Nakamura. 2020. Psnet: A style transfer network for point cloud stylization on geometry and color. In *IEEE Winter Conference on Applications of Computer Vision (WACV)*.
- Dongdong Chen, Jing Liao, Lu Yuan, Nenghai Yu, and Gang Hua. 2017. Coherent online video style transfer. In *IEEE International Conference on Computer Vision (ICCV)*.
- Xinghao Chen, Yiman Zhang, Yunhe Wang, Han Shu, Chunjing Xu, and Chang Xu. 2020. Optical flow distillation: Towards efficient and stable video style transfer. In *European Conference on Computer Vision (ECCV)*.
- Yingying Deng, Fan Tang, Weiming Dong, haibin Huang, Ma chongyang, and Changsheng Xu. 2021. Arbitrary Video Style Transfer via Multi-Channel Correlation. In *AAAI*.
- Andrew Fitzgibbon, Yonatan Wexler, and Andrew Zisserman. 2005. Image-based rendering using image-based priors. *International Journal of Computer Vision (IJCV)* (2005).
- Pascal Fua and Yvan G Leclerc. 1995. Object-centered surface reconstruction: Combining multi-image stereo and shading. *International Journal of Computer Vision (IJCV)* (1995).
- Chang Gao, Derun Gu, Fangjun Zhang, and Yizhou Yu. 2018. Reconet: Real-time coherent video style transfer network. In *Asian Conference on Computer Vision (ACCV)*.
- Wei Gao, Yijun Li, Yihang Yin, and Ming-Hsuan Yang. 2020. Fast video multi-style transfer. In *IEEE Winter Conference on Applications of Computer Vision (WACV)*.
- Stephan J Garbin, Marek Kowalski, Matthew Johnson, Jamie Shotton, and Julien Valentin. 2021. FastNeRF: High-Fidelity Neural Rendering at 200FPS. *arXiv preprint arXiv:2103.10380* (2021).
- Leon A Gatys, Alexander S Ecker, and Matthias Bethge. 2016. Image style transfer using convolutional neural networks. In *IEEE Conference on Computer Vision and Pattern Recognition (CVPR)*.
- Thibault Groueix, Matthew Fisher, Vladimir G Kim, Bryan C Russell, and Mathieu Aubry. 2018. A papier-mâché approach to learning 3d surface generation. In *IEEE Conference on Computer Vision and Pattern Recognition (CVPR)*.
- Agrim Gupta, Justin Johnson, Alexandre Alahi, and Li Fei-Fei. 2017. Characterizing and improving stability in neural style transfer. In *IEEE International Conference on Computer Vision (ICCV)*.
- David Ha, Andrew Dai, and Quoc V Le. 2016. Hypernetworks. *arXiv preprint arXiv:1609.09106* (2016).
- Paul Henderson and Vittorio Ferrari. 2019. Learning single-image 3d reconstruction by generative modelling of shape, pose and shading. *International Journal of Computer Vision (IJCV)* (2019).
- Haozhi Huang, Hao Wang, Wenhan Luo, Lin Ma, Wenhao Jiang, Xiaolong Zhu, Zhifeng Li, and Wei Liu. 2017. Real-time neural style transfer for videos. In *IEEE Conference on Computer Vision and Pattern Recognition (CVPR)*.
- Xun Huang and Serge Belongie. 2017. Arbitrary style transfer in real-time with adaptive instance normalization. In *IEEE International Conference on Computer Vision (ICCV)*.
- Eddy Ilg, Nikolaus Mayer, Tommy Saikia, Margret Keuper, Alexey Dosovitskiy, and Thomas Brox. 2017. FlowNet 2.0: Evolution of optical flow estimation with deep networks. In *IEEE Conference on Computer Vision and Pattern Recognition (CVPR)*.
- Justin Johnson, Alexandre Alahi, and Li Fei-Fei. 2016. Perceptual losses for real-time style transfer and super-resolution. In *European Conference on Computer Vision (ECCV)*.
- Angjoo Kanazawa, Shubham Tulsiani, Alexei A Efros, and Jitendra Malik. 2018. Learning category-specific mesh reconstruction from image collections. In *European Conference on Computer Vision (ECCV)*.
- Hiroharu Kato, Yoshitaka Ushiku, and Tatsuya Harada. 2018. Neural 3d mesh renderer. In *Proceedings of the IEEE conference on computer vision and pattern recognition*. 3907–3916.
- Diederik P Kingma and Max Welling. 2014. Auto-encoding variational bayes. In *International Conference on Learning Representations (ICLR)*.
- Arno Knapitsch, Jaesik Park, Qian-Yi Zhou, and Vladlen Koltun. 2017. Tanks and Temples: Benchmarking Large-Scale Scene Reconstruction. *ACM Transactions on Graphics* (2017).
- Kiriakos N Kutulakos and Steven M Seitz. 2000. A theory of shape by space carving. *International Journal of Computer Vision (IJCV)* (2000).
- Wei-Sheng Lai, Jia-Bin Huang, Oliver Wang, Eli Shechtman, Ersin Yumer, and Ming-Hsuan Yang. 2018. Learning blind video temporal consistency. In *European Conference on Computer Vision (ECCV)*.
- Xueting Li, Sifei Liu, Jan Kautz, and Ming-Hsuan Yang. 2018. Learning linear transformations for fast arbitrary style transfer. In *IEEE Conference on Computer Vision and Pattern Recognition (CVPR)*.
- Yijun Li, Chen Fang, Jimei Yang, Zhaowen Wang, Xin Lu, and Ming-Hsuan Yang. 2017a. Diversified texture synthesis with feed-forward networks. In *IEEE Conference on Computer Vision and Pattern Recognition (CVPR)*.
- Yijun Li, Chen Fang, Jimei Yang, Zhaowen Wang, Xin Lu, and Ming-Hsuan Yang. 2017b. Universal style transfer via feature transforms. In *Advances in Neural Information Processing Systems (NeurIPS)*.
- Yanghao Li, Naiyan Wang, Jiaying Liu, and Xiaodi Hou. 2017c. Demystifying neural style transfer. *arXiv preprint arXiv:1701.01036* (2017).
- Chen-Hsuan Lin, Chen Kong, and Simon Lucey. 2018. Learning efficient point cloud generation for dense 3d object reconstruction. In *AAAI Conference on Artificial Intelligence (AAAI)*.
- Ben Mildenhall, Pratul P Srinivasan, Matthew Tancik, Jonathan T Barron, Ravi Ramamoorthi, and Ren Ng. 2020. Nerf: Representing scenes as neural radiance fields for view synthesis. In *European Conference on Computer Vision (ECCV)*. Springer.
- Kiri Nichol. 2016. Painter by numbers, wikiart. <https://www.kaggle.com/c/painter-by-numbers>
- Jhony K Pontes, Chen Kong, Sridha Sridharan, Simon Lucey, Anders Eriksson, and Clinton Fookes. 2018. Image2mesh: A learning framework for single image 3d reconstruction. In *Asian Conference on Computer Vision (ACCV)*.
- Emil Praun, Adam Finkelstein, and Hugues Hoppe. 2000. Lapped textures. In *Computer graphics and interactive techniques*.
- Gernot Riegler and Vladlen Koltun. 2020a. Free view synthesis. In *European Conference on Computer Vision (ECCV)*.
- Gernot Riegler and Vladlen Koltun. 2020b. Stable View Synthesis. In *IEEE Conference on Computer Vision and Pattern Recognition (CVPR)*.
- Johannes L Schonberger and Jan-Michael Frahm. 2016. Structure-from-motion revisited. In *Proceedings of the IEEE conference on computer vision and pattern recognition*.
- Johannes Lutz Schönberger, Enliang Zheng, Marc Pollefeys, and Jan-Michael Frahm. 2016. Pixelwise View Selection for Unstructured Multi-View Stereo. In *European Conference on Computer Vision (ECCV)*.
- Katja Schwarz, Yiyi Liao, Michael Niemeyer, and Andreas Geiger. 2020. Graf: Generative radiance fields for 3d-aware image synthesis. *arXiv preprint arXiv:2007.02442* (2020).
- Steven M Seitz, Brian Curless, James Diebel, Daniel Scharstein, and Richard Szeliski. 2006. A comparison and evaluation of multi-view stereo reconstruction algorithms. In *IEEE Conference on Computer Vision and Pattern Recognition (CVPR)*.
- Falong Shen, Shuicheng Yan, and Gang Zeng. 2018. Neural style transfer via meta networks. In *IEEE Conference on Computer Vision and Pattern Recognition (CVPR)*.
- Karen Simonyan and Andrew Zisserman. 2015. Very Deep Convolutional Networks for Large-Scale Image Recognition. In *International Conference on Learning Representations (ICLR)*.
- Peter Sturm and Bill Triggs. 1996. A factorization based algorithm for multi-image projective structure and motion. In *European Conference on Computer Vision (ECCV)*. Springer.
- Jan Svoboda, Asha Anosheh, Christian Osendorfer, and Jonathan Masci. 2020. Two-stage peer-regularized feature recombination for arbitrary image style transfer. In *IEEE Conference on Computer Vision and Pattern Recognition (CVPR)*.
- Dmitry Ulyanov, Vadim Lebedev, Andrea Vedaldi, and Victor S Lempitsky. 2016. Texture Networks: Feed-forward Synthesis of Textures and Stylized Images. In *International Conference on Machine Learning (ICML)*.
- Wenjing Wang, Jizheng Xu, Li Zhang, Yue Wang, and Jiaying Liu. 2020a. Consistent video style transfer via compound regularization. In *AAAI Conference on Artificial Intelligence (AAAI)*.
- Wenjing Wang, Shuai Yang, Jizheng Xu, and Jiaying Liu. 2020b. Consistent Video Style Transfer via Relaxation and Regularization. *IEEE Transactions on Image Processing (TIP)* (2020).
- Xide Xia, Tianfan Xue, Wei-sheng Lai, Zheng Sun, Abby Chang, Brian Kulis, and Jiawen Chen. 2021. Real-time Localized Photorealistic Video Style Transfer. In *WACV*.
- Fanbo Xiang, Zexiang Xu, Miloš Hašan, Yannick Hold-Geoffroy, Kalyan Sunkavalli, and Hao Su. 2021. NeuTex: Neural Texture Mapping for Volumetric Neural Rendering. *arXiv preprint arXiv:2103.00762* (2021).
- Alex Yu, Vickie Ye, Matthew Tancik, and Angjoo Kanazawa. 2021. pixelNeRF: Neural Radiance Fields from One or Few Images. *IEEE Conference on Computer Vision and Pattern Recognition (CVPR)* (2021).
- Kai Zhang, Gernot Riegler, Noah Snavely, and Vladlen Koltun. 2020. Nerf++: Analyzing and improving neural radiance fields. *arXiv preprint arXiv:2010.07492* (2020).